Incorporation of Cascaded Metallic Gratings into Thin Film Solar Cells for Broadband Plasmonic Light Trapping

Long Wen, **Fuhe Sun**, **and Qin Chen**
Key Laboratory of Nanodevices and Applications-CAS
Collaborative Innovation Center of Suzhou Nano Science and Technology
Suzhou Institute of Nano-Tech and Nano-Bionics, Chinese Academy of Sciences (CAS)
Suzhou 215123, China

(*Invited Paper*)

Abstract— Plasmonic nanostructures have been regarded as a promising light trapping strategy towards boosting solar cell efficiency recently. However, the absorption enhancement stemming from surface plasmon excitations always suffers from an inherent limitation of narrow bandwidths, which may hamper the complete utilization of the solar radiation in a broadband spectrum for solar cells. In this paper, we theoretically show that by cascading metal gratings with different sizes atop the amorphous Silicon thin film solar cells (TFSCs), the enhanced light absorption band of the ultrathin active layer is extended due to the excitation of multiple localized surface plasmon resonances (LSPRs). For one-dimensional (1D) cascaded grating structure, the metallic gratings with different widths act as discrete nanoantennas which independently and efficiently collect the incoming photons at the LSPR wavelengths, leads to an enhancement of 60% in photocurrent for the TM-polarized incident illumination. Furthermore, it appears that both the coupling of plasmonic/photonic modes and their inter-coupling effects contribute to the light trapping in the 2D cascaded grating structures, which leads to an enhancement of 66.5% in the photocurrent over the bare TFSCs.

1. INTRODUCTION

In the past few years, the field of plasmonics has emerged as a rapidly expanding new area in photonics, with researchers exploring its potential applications in photovoltaics, biochemical sensing and optical computing [1–4]. Surface plasmon effects stemming from the collective oscillations of electromagnetic waves and free electrons at metal/dielectric interfaces, provide an effective method to manipulate and concentrate light into the nanoscale. The localized surface plasmons resonance (LSPR) excited in metal nanostructures and surface plasmon polaritons (SPPs) propagating at the metal/semiconductor interface are found to greatly enhance the absorption of semiconductors [2–5]. Beside the benefits of near-field light concentration, plasmonic nanostructures can serve as scattering objects [2, 5, 6] or photonic mode couplers [7, 8] to trap light more efficiently into the photoactive semiconductor with a elongated light path length. These unique optical properties associated with plasmonic structures render them promising light trapping elements for the next generation thin-film solar cells (TFSCs).

Previous studies have shown that the performance of the TFSCs can be improved considerably by incorporating randomly distributed metal nanoparticles [5, 6] or nanopatterned metal layers [7–9] on the front or rear side of the cells. Although the former structures are fabricated using relatively cheap self-assemble technologies, they suffer from limited spatial control of sharps or positions of the metallic nanoparticles, which may result in high level of parasitic losses in the metal. In contrast, the latter enables precisely patterning the metal elements and therefore engineering the plasmonic resonances. Nevertheless, such a single layer metallic patterns suffers inherently narrow bandwidths of surface plasmon excitations, which does not meet the requirement for broadband absorption enhancement. With the aim of extending the plasmonic light trapping over a broadband spectrum, researchers have proposed the dual plasmonic structures containing metallic patterns on both front and rear side of the active layer [10, 11]. However, the increased complexity in fabrication as well as the sensitivity to the lateral offset between the front and back metal elements makes this approach less attractive. In this paper, we present that by cascading metallic gratings with different sizes atop the TFSCs, the absorption in the ultrathin absorber is enhanced in an extended spectral band due to the excitation of multiple LSPRs. It was found that our proof-of-concept amorphous silicon (a-Si) TFSC containing one-dimensional (1D) cascaded gratings enables an enhancement of 60% in photocurrent over the reference cell under the TM-polarized incident illumination. When

incorporating with 2D cascaded gratings, the coexistence and coupling of cascaded LSPRs and photonic modes were identified as gain mechanisms of light absorption in TFSCs.

As the LSPR behavior is exquisitely sensitive to the geometrical parameters of metallic nanostructures [7, 12], we adopt it as a platform in present work to construct our cascaded plasmonic light trapping TFSCs. As shown in Figure 1(a), we began with a simple front grating TFSCs consisting of a periodic array of 1D Ag gratings on a silica-coated 50 nm thick a-Si film followed by a 300 nm thick Ag as a reflective mirror. We will refer to this single-sized grating structure as non-cascaded TFSC in the following. Normally incident sunlight with TM polarizations is considered for the purpose of excitation of LSPR. From Figure 1(a) (bottom), the strong localized feature observed in the normalized magnetic field gives a direct evidence of the excitation of LSPR in the non-cascaded TFSCs. The calculated absorption spectra in the active layer are plotted in Figure 1(b). It is found that the reference TFSC in absence of gratings exhibits poor absorption ability, especially in the longer wavelengths. The non-cascaded TFSC have higher absorption in most wavelengths as compared with the reference cell. At wavelengths near LSPR, we observe a narrow peak exhibiting high enhancements up to 8 for the non-cascaded TFSCs. However, the absorption quickly decreases to 50% at a wavelength of 25 nm away from the peak because of the strong resonant nature of LSPR.

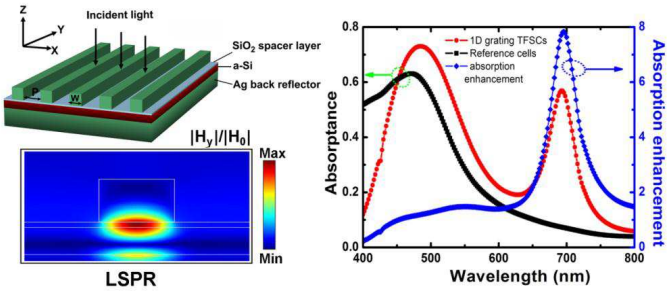

Figure 1: (a) Schematic of the 1D non-cascaded TFSC (top) and the LSPR H-field intensity distribution in the XZ plane for a non-cascaded TFSC with the grating width of 120 nm and period of 360 nm (bottom). (b) The absorption spectra of the non-cascaded TFSC and the reference TFSC. The absorption enhancement from the non-cascaded TFSC is also given.

Figure 2(a) shows the contour plots of the calculated light absorption in a-Si layer of the non-cascaded TFSCs as a function of the incident wavelength and the grating width. Two strong absorption bands can be distinguished. The first band around 400–500 nm for the grating widths smaller than 60 nm can be attributed to the longitudinal Fabry-Perot (FP) cavity modes supported by the air/a-Si/Ag cavity. As it is inherent to the flat stacks, this band does not significantly enhance the absorption over the reference TFSCs. With the increasing grating width, the resonance wavelength of the cavity mode has a red-shift owning to the coupling with the transverse propagation SPP modes. The second strong absorption band represents the LSPR excitation extends its resonance wavelengths through 350 nm to 780 nm and overlaps with the first absorption band at the wavelengths around 470 nm leading to the strongest absorption. With the strong light localization, the LSPR band gives rise to absorption enhancement factors up to 3.6 and 8 for gratings with widths of 80 and 120 nm at their resonant wavelengths. Figure 2(b) shows the a-Si absorption of the non-cascaded TFSCs at the different reciprocal lattice constants, $G = 2\pi/P$ with a fixed grating width of 100 nm. It is found that the position of the LSPR band is insensitive with the grating periods but its amplitude decrease slightly towards larger periods. Nevertheless, even for gratings with a large period of 900 nm, the LSPR induced absorption enhancement still maintains a high value of 3.2. Finally, several other trivial features observed in Figures 2(a), (b) are marked by white circles, black and red dashed lines, which represent respectively the excitation of Wood's anomalies and the bound SPPs at the Ag/SiO_2 and Ag/Air interfaces.

The broadband excitation of LSPRs by simply manipulating the widths of grating provides a large free degree in designing of the cascaded grating systems. Keeping the LSPRs in the weak absorption band of the a-Si, four gratings with the widths $W = 60$, 80, 100, and 120 nm are chosen to construct the 1D cascaded TFSCs. As shown in Figure 2(d), the multi-sized gratings serve as four discrete LSPR resonators patterned side by side with a lateral spacing of 120 nm. Figure 2(c)

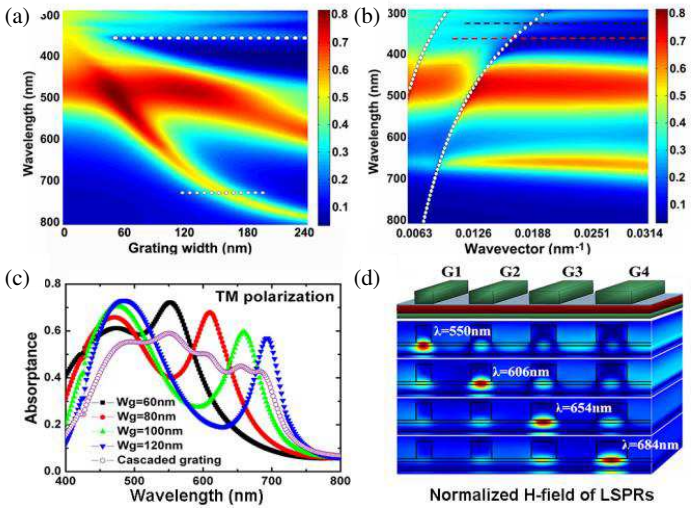

Figure 2: Contour plots of the a-Si absorption spectra as a function of (b) the grating width ($P = 360\,\text{nm}$) and (c) the reciprocal lattice vector of the 1D gratings ($W = 100\,\text{nm}$). (c) a-Si absorption spectra of the cascaded and non-cascaded TFSCs under TM-polarized illumination. (d) Schematic of 1D cascaded TFSC and the H-field profiles of the cascaded TFSCs at four LSPR wavelengths.

shows the absorption of a-Si in the cascaded and non-cascaded ($P = 240\,\text{nm}$) TFSCs with different grating widths ($W = 60,\ 80,\ 100,\ 120\,\text{nm}$). In consistent with the LSPR induced absorption peaks observed in the regular non-cascaded cells, four resonance peaks can be distinguished from the absorption spectrum of the cascaded TFSCs. Compared to the non-cascaded structures, the cascaded TFSCs significantly broaden the absorption band because of the simultaneous excitations of multiple LSPRs. As confirmed by the normalized H-field patterns shown in Figure 3(c), G1, G2, G3, and G4 act as four independent resonators with their resonances localized in specific positions. Considering the AM1.5G spectrum, we calculated the integrated photocurrent enhancement for the cascaded TFSCs over the reference structure. It is found that the cascaded structure gives rise to an enhancement of 60% in photocurrent for the TM-polarized illumination. As the enhancement mainly attribute to the simultaneous excitations of multiple LSPRs, broadband angle-insensitive enhancement can be expected in the cascaded TFSCs. Figure 3(a) shows the absorptance of the 1D cascaded TFSC under normal and oblique light incidence (30 degree). For the two different incident angles, we observed almost identical absorption spectra. Figure 3(b) presents the photocurrent enhancement as a function of the incident angle for TM polarizations. At an angles around 15°, the maximum enhancement of ~ 1.68 is observed. It can be seen that the cascaded design exhibits photocurrent enhancement for angles up to 60°, confirming that the cascaded TFSC allows for broadband angle-independent light absorption.

Until now, we have mainly focused on the 1D cascaded grating configurations under the TM-polarized illumination. However, to account for the randomly polarized nature of sunlight, both the polarizations need to be considered. At TE-polarized illumination, a significant part of incoming light is directly blocked by the front metallic gratings, resulting in a significantly suppressed absorption in the 1D cascaded TFSC referred in Figures 3, 4. In the following, we will extend

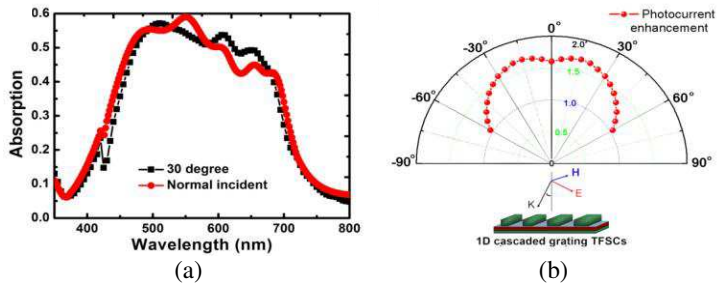

Figure 3: (a) Absorption spectra of 1D cascaded TFSCs under normal and oblique light incidence. (b) Photocurrent enhancement as a function of the angle of incidence for TM polarization.

our considerations into the 2D grating patterned TFSCs, in which an array of Ag nanocubes arranged into a rectangle lattice was employed to achieve the polarization insensitive performance. By breaking the continuity of 1D grating and shrinking its length (W_y) in the direction parallel to grating groove, the physical mechanisms involved in geometric transformation from 1D to 2D grating structures can be distinguished in a straightforward and intuitive manner. The schematic of 2D non-cascaded TFSC is shown in Figure 4(a), the grating width in the x-direction is fixed to 80 nm, the grating periods in the x and y-direction are fixed to 360 nm, and the thickness of SiO_2 spacer layer is charged to 20 nm for the sake of more efficiently excite of LSPR for 2D coupler. As shown in Figure 4(b), the absorption spectra of TFSCs under TM-polarized illumination hold their general profiles with gradually and mildly decreasing in absorption as 1D gratings change to 2D cuboids. Besides to the aforementioned cavity mode and LSPR (marked as peak A and B), two new weak peaks (marked as C_1 and C_2) emerged for the smaller W_y values, which are attributed to the fundamental TE waveguide mode resonances excited by the G [10] and G [11] grating diffractions.

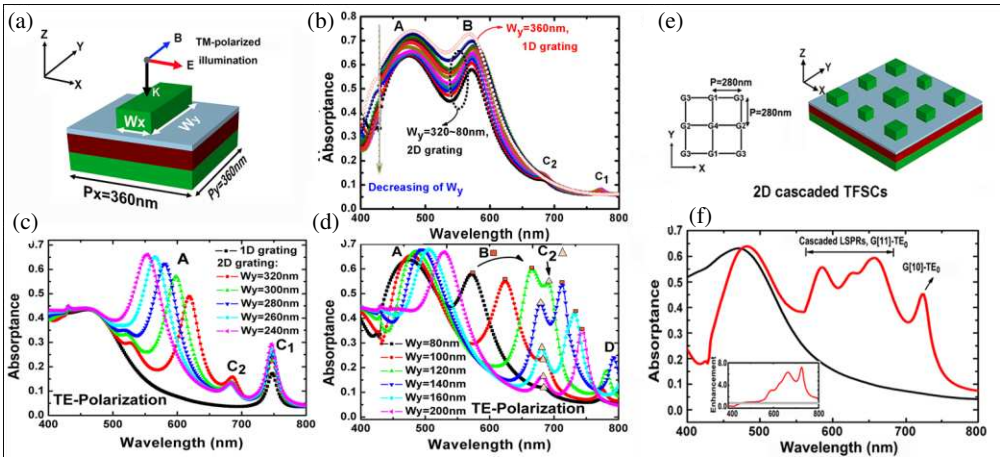

Figure 4: (a) Schematic of 2D non-cascaded TFSC. (b)–(d) Calculated a-Si absorption spectra of 2D non-cascaded TFSCs with different W_y: (b) Results for TM-polarized illumination; (c), (d) Results for TE-polarized illumination. (e) Schematic of 2D cascaded TFSC. (f) Absorption spectra and enhancement in absorption of the 2D cascaded grating TFSC.

Under TE-polarized illumination, it is found that the shrinking of W_y leads to a more complex evolution of the absorption spectra as the LSPRs shift their resonance positions and opt to couple with the photonic modes. In order to make a clear illustration, the absorption spectra is divided into two length regions (W_y = 360–240 nm and W_y = 200–80 nm) corresponding to Figures 4(c), (d). As depicted in the Figure 2(a), we have observed that the position of LSPR for the grating width of 240 nm is close to the red end of the spectrum. Consequently, for W_y larger than 240 nm, no LSPR related absorption peak was observed in Figure 4(c). For W_y larger than 240 nm, C_1 and C_2 peaks referred as two grating coupled waveguide modes have higher absorption as compared with the peaks under TM illumination owing to the elongated confinement of the modal fields beneath the gratings along the y direction. In addition, a sharp and pronounced peak A emerges even for a very small slit width in the y direction. The increase of W_y leads to a significant red-shift of the peak A, which may imply a different origin from the peak A for TM illumination (longitudinal FP cavity mode). For W_y smaller than 200 nm, the LSPR peaks can be observed in the absorption spectra (Figure 4(d)). In consistent with the results of 1D structures, the LSPR peak wavelengths decrease with the W_y. We noticed that C_1 peak is absent in this figure (except for W_y = 80 nm). It appears that the shrinking of W_y leads to a slight red-shift and a decrease of the modal confinement of the waveguide resonance. Thus, one may expect that the peak C_1 is swamped by other peaks. Interestingly, when the LSPR and C_2 peaks approach, their resonances are significantly enhanced due to the formation of a waveguide-plasmon-polariton [7]. The strong coupling between the LSPR and the waveguide modes also can be confirmed by the shifted C_2 resonance for W_y = 120 nm, where the absorption enhancement of C_2 resonance peak is 9.5, much higher than the pure waveguide mode. The newly emerged peak D red shifts its resonance with the increasing W_y, which we attribute to the longitudinal FP cavity mode supported by grating patterned slabs. According to the effective medium theory, the significantly divergence between

peak D and the aforementioned peak A can be understood by regarding the strong anisotropic refractive index of gratings under the TE and TM-polarized incidence.

To achieve the cascading LSPR enhancement, four 2D LSPR resonators with different grating widths of 80, 100, 110, 120 nm are incorporated in the cascaded TFSCs, as depicted in Figure 4(e). The 2D cuboids are arranged squarely with a period of 280 nm. For this period, both first grating order and the diagonal order coupled waveguide modes interact efficiently with the LSPRs. Figure 4(b) shows the absorption spectra and the enhancement of the proposed 2D cascaded TFSCs. Multiple absorption peaks related to LSPRs cascading and waveguide modes coupling can clearly be identified in the absorption spectra of the cells. It is very remarkable that a broadband enhancement can be achieved for the spectral range of 550–750 nm as shown in the inset of Figure 4(f). By integrating the AM1.5G solar spectral photocurrent in the case of a non-polarized illumination, we found that the 2D cascaded TFSCs gives rise to a 66.5% increase in the photocurrent over the reference structure.

In conclusion, we proposed a cascaded design based on integrating multi-sized plasmonic resonators for enhancing the optical absorption in ultra-thin TFSCs, beyond the limit of regular non-cascaded structures. We numerically demonstrated that the cascaded TFSC enable the excitations of multiple LSPRs in a broad wavelength region due to the presence of multi-sized front gratings. In addition, the coexistence and coupling of cascaded LSPRs and photonic modes further contributes to the optical absorption enhancement leading to an enhancement of 66.5% in the photocurrent in the 2D cascaded TFSC.

ACKNOWLEDGMENT

This work was supported by the grants from the National Natural Science Foundation of China (Grant Nos. 11274344), the Hundred Talents Program of Chinese Academy of Sciences, the Scientific Research Foundation for the Returned Overseas Chinese Scholars, State Education Ministry.

REFERENCES

1. Schuller, J. A., E. S. Barnard, W. Cai, Y. C. Jun, J. S. White, and M. Brongersma, "Plasmonics for extreme light concentration and manipulation," *Nat. Mater.*, Vol. 9, 193–204, 2010.
2. Atwater, H. A. and A. Polman, "Plasmonics for improved photovoltaic devices," *Nat. Mater.*, Vol. 9, 205–213, 2010.
3. Feng, J., V. S. Siu, A. Roelke, V. Mehta, S. Y. Rhieu, G. T. Palmore, and D. Pacifici, "Nanoscale plasmonic interferometers for multispectral, high-throughput biochemical sensing," *Nano Lett.*, Vol. 8, 602-9, 2012.
4. Lu, C., X. Hu, H. Yang, and Q. Gong, "Integrated all-optical logic discriminators based on plasmonic bandgap engineering," *Sci. Rep.*, Vol. 3, 2778-7, 2013.
5. Spinelli, P., V. E. Ferry, J. Van de Groep, M. Van Lare, M. A. Verschuuren, R. E. I. Schropp, H. A. Atwater, and A. Polman, "Plasmonic light trapping in thin-film Si solar cells," *J. Opt.*, Vol. 14, 024002, 2012.
6. Pillai, S., K. R. Catchpole, T. Trupke, and M. A. Green, "Surface plasmon enhanced silicon solar cells," *J. Appl. Phys.*, Vol. 101, 093105, 2007.
7. Pala, R. A., J. White, E. Barnard, J. Liu, and M. L. Brongersma, "Design of plasmonic thin-film solar cells with broadband absorption enhancements," *Adv. Mater.*, Vol, 21, 3504–3509, 2009.
8. Pala, R. A., J. S. Q. Liu, E. S. Barnard, D. Askarov, E. C. Garnett, S. Fan, and M. L. Brongersma, "Optimization of non-periodic plasmonic light-trapping layers for thin-film solar cells," *Nat. Mater.*, Vol. 4, 2095, 2013.
9. Ferry, V. E., M. A. Verschuuren, H. B. T. Li, E. Verhagen, R. J. Walters, R. E. I. Schropp, H. A. Atwater, and A. Polman, "Light trapping in ultrathin plasmonic solar cells," *Opt. Express*, Vol. 18, A237–A245, 2010.
10. Sefunc, M. A., A. K. Okyay, and H. V. Demir, "Volumetric plasmonic resonator architecture for thin-film solar cells," *Appl. Phys. Lett.*, Vol. 98, 093117, 2011.
11. Shen, H. and B. Maes, "Combined plasmonic gratings in organic solar cells," *Opt. Express*, Vol. 19, A1202–A1210, 2011.
12. Munday, J. N. and H. A. Atwater, "Large integrated absorption enhancement in plasmonic solar cells by combining metallic gratings and antireflection coatings," *Nano Lett.*, Vol. 11, 2195–2201, 2011.